

Synthesis and Electrochemical Properties of Oxovanadium Complexes with a Pentadentate Schiff Base Ligand

Masanobu Tsuchimoto,* Toshio Ishii,[1] Takane Imaoka,[2] and Kimihisa Yamamoto[2]

Department of Life and Environmental Sciences, Chiba Institute of Technology, Shibazono 2-1-1, Narashino, Chiba 275-0023

[1]Department of Mechanical Engineering, Chiba Institute of Technology, Shibazono 2-1-1, Narashino, Chiba 275-0023

[2]Department of Chemistry, Faculty of Science and Technology, Keio University, Hiyoshi 3-14-1, Kohoku-ku, Yokohama 223-8522

Received February 27, 2004; E-mail: tmoto@pf.it-chiba.ac.jp

Oxovanadium(IV) and (V) complexes with a pentadentate Schiff base ligand, $[V^{IV}O(HL)]\cdot H_2O$ {H_3L: *N*,*N*′-bis(3-ethoxysalicylidene)-2-hydroxy-1,3-propanediamine} and $[V^{V}O(L)]\cdot CH_3CN$, were prepared by the reaction of the Schiff base ligand with $[V^{IV}O(acac)_2]$ (H_2acac: acetylacetone) in CH_3CN under an argon atmosphere and in air, respectively. IR data of the complexes indicate that $[V^{IV}O(HL)]$ and $[V^{V}O(L)]$ have polymeric (···V=O···V=O···) and monomeric structures, respectively, in the solid state. An X-ray crystal structure analysis of $[V^{V}O(L)]\cdot CH_3CN$ was carried out. The complex has a distorted octahedral structure with one of the imine nitrogen atoms trans to the oxo atom. The cyclic voltammogram of $[V^{V}O(L)]$ in CH_2Cl_2 shows a quasi-reversible V(V)/V(IV) redox couple with $E_{1/2} = -0.74$ V vs Ag/Ag^+. On the other hand, the cyclic voltammogram of $[V^{IV}O(HL)]$ in CH_2Cl_2 shows two irreversible oxidation waves at +0.23 and +0.33 V with a scan rate 100 mV/s. The cyclic voltammogram of $[V^{IV}O(HL)]$ in DMSO shows a quasi-reversible V(V)/V(IV) redox couple with $E_{1/2} = -0.05$ V. Electrochemcal data indicate that $[V^{IV}O(HL)]$ form dimeric species in a weakly Lewis basic solvent by coodination of the alcohol group to the vanadium atom of the adjacent molecule.

The structures and electrochemistry of oxovanadium(IV) and (V) complexes with tetradentate Schiff base ligands have been extensively studied to this day. Usually, most oxovanadium(IV) complexes with a tetradentate Schiff base ligand are known to have monomeric square-pyramidal structures or polymeric linear chain structures (···V=O···V=O···) in the solid state.[1,2] The IR spectra of the monomeric complexes, like $[V^{IV}O(salen)]$ (H_2salen: *N*,*N*′-disalicylidene-1,2-ethanediamine), show a V=O stretching band around 970 cm^{-1}, and those of the polymeric complexes, like $[V^{IV}O(salpn)]$ (H_2salpn: *N*,*N*′-disalicylidene-1,3-propanediamine), show a V=O stretching band around 860 cm^{-1}.[1,2] Most oxovanadium(V) complexes with a tetradentate Schiff base ligand are monomeric, and the complexes have distorted octahedral structures with the weak coordination of a solvent molecule,[3] or a counter ion[4–6] *trans* to the oxo ligand. The IR spectra of the monomeric oxovanadium(V) complexes show a V=O stretching band at around 970 cm^{-1}. An IR spectrum of a polymeric oxovanadium(V) complex, $[V^{V}O(5\text{-MeOsalen})]SbF_6$ {$H_2$5-MeOsalen: *N*,*N*′-bis(5-methoxysalicylidene)-1,2-ethanediamine} shows a V=O stretching band at 878 cm^{-1}.[6] Cyclic voltammograms of oxovanadium(IV) and (V) complexes with a tetradentate Schiff base ligand usually show a reversible V(V)/V(IV) redox wave in the range between −0.1 and +0.4 V vs Ag/Ag^+ in organic solvents (CH_3CN, CH_2Cl_2, DMSO).[4,7–11] On the other hand, in strongly acidic solutions, $[V^{IV}O(salen)]$ forms dimeric μ-oxo (V–O–V) complexes,[7,12,13] and the voltammograms of the complexes show multi-electron redox process.[7,12,14,15]

However, little is known about the structures and electrochemistry of oxovanadium complexes with a pentadentate Schiff base ligand, like H_3L {H_3L: *N*,*N*′-bis(3-ethoxysalicylidene)-2-hydroxy-1,3-propanediamine, Fig. 1}. In this study, oxovanadium(IV) and (V) complexes with the Schiff base ligand, $[V^{IV}O(HL)]$ and $[V^{V}O(L)]$ were prepared, and their electrochemical properties were investigated.

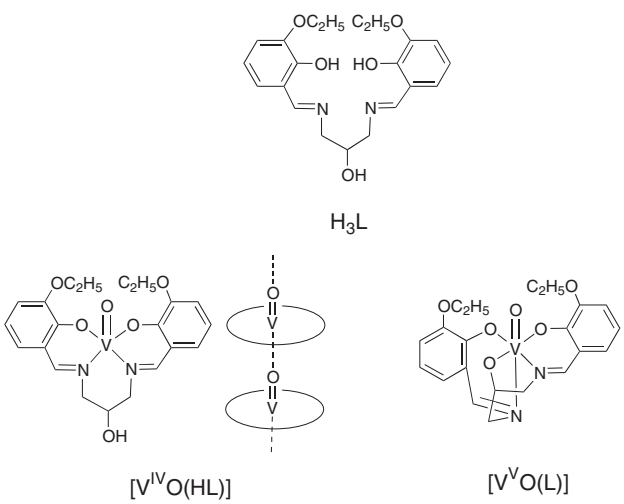

Fig. 1. H_3L, $[V^{IV}O(HL)]$, and $[V^{V}O(L)]$.

Published on the web October 9, 2004; DOI 10.1246/bcsj.77.1849

Results and Discussion

Preparation of the Complexes. The reaction of H_3L with $[V^{IV}O(acac)_2]$ in CH_3CN under an argon atmosphere yielded a brown oxovanadium(IV) complex, $[V^{IV}O(HL)]\cdot H_2O$. On the other hand, the reaction of H_3L with $[V^{IV}O(acac)_2]$ in air yielded dark-blue crystals of an oxovanadium(V) complex, $[V^{V}O(L)]\cdot CH_3CN$. The IR spectra of $[V^{IV}O(HL)]$ and $[V^{V}O(L)]$ show a V=O stretching band at 857 and 947 cm^{-1}, respectively. Tetradentate Schff base–oxovanadium(IV) and (V) complexes generally show a V=O stretching band around 860 cm^{-1} for polymeric structures,[1,2,6] and around 970 cm^{-1} for monomeric structures.[3–6] Thus, $[V^{IV}O(HL)]$ and $[V^{V}O(L)]$ are assigned to polymeric (···V=O···V=O···) and monomeric structures, respectively, in the solid state. In $[V^{IV}O(HL)]$, the ligand HL is supposed to coordinate to the vanadium atom with the two imine nitrogen and two phenolate oxygen atoms. The oxygen atom of the alcohol group will not coordinate to the vanadium atom in the solid state (Fig. 1). In $[V^{V}O(L)]$, the ligand L is supposed to coordinate to the vanadium atom with the two imine nitrogen, two phenolate oxygen, and alcoholate oxygen atoms. Elemental analyses indicate the presence of crystal water and CH_3CN in the crystals of $[V^{IV}O(HL)]$ and $[V^{V}O(L)]$, respectively. The oxovanadium(IV) and (V) complexes, $[V^{IV}O(HL)]$ and $[V^{V}O(L)]$, are stable in the solid state at room temperature. However, both of the complexes are not very stable in solutions. A brown CH_3CN solution of $[V^{IV}O(HL)]$ gradually turned dark blue by standing in air. The oxovanadium(V) complex $[V^{V}O(L)]$ gradually decomposed in solutions at room temperature, especially in ones containing water.[16]

An X-ray crystal structure analysis of $[V^{V}O(L)]\cdot CH_3CN$ was carried out. An ORTEP drawing is shown in Fig. 2. The complex is monomeric, and all of the imine nitrogen, phenolate oxygen, and alcoholate oxygen atoms in the Schiff base ligand coordinate to the vanadium atom. The complex has a distorted octahedral structure with one of the imine nitrogen atoms trans to the oxo atom. The V(1)–O(2) and V(1)–N(8) distances are 1.599(2) and 2.241(2) Å, respectively. The V(1)–N(8) distance (2.241(2) Å) is longer than the V(1)–N(9) distance (2.110(2) Å). A strong trans influence of the oxo ligand affects the elongation of the vanadium–nitrogen distance trans to the oxo atom. On the other hand, the NMR spectra of $[V^{V}O(L)]$ indicate the presence of a different structure in solutions. The ^{13}C NMR spectrum of $[V^{V}O(L)]$ in CD_2Cl_2 shows nine signals at $\delta = 163.0$, 156.5, 147.2, 124.1, 119.9, 119.8 (Ar and N=CH–C), 80.6 (–OCH(CH_2–)$_2$), 65.8 (N–CH_2–C and O–CH_2–C), 15.3 (CH_3).[16] The ^1H NMR spectrum of the complex in CD_2Cl_2 shows a methyl proton signal at $\delta = 1.30$ (t, 7 Hz). The ^1H NMR spectra of the complex in CD_3CN and in DMSO-d_6 also show a methyl proton signal at $\delta = 1.26$ (t, 7 Hz) and at $\delta = 1.19$ (t, 7 Hz), respectively. The structure of $[V^{V}O(L)]$ in solutions, estimated from the NMR spectra (C_2 or C_s symmetry), does not coincident with the crystal structure of the complex determined from the X-ray structure analysis (C_1 symmetry). Molecular models suggest that the structurally possible, less-strained isomer in solutions is the *trans-oxo-O* isomer (C_s symmetry) (Fig. 3). There may be equilibrium between the *trans-oxo-O* isomer (C_s symmetry) and the *trans-oxo-N* isomer (C_1 symmetry) in solutions. Because the *trans-oxo-O* isomer is far more stable than the *trans-oxo-N* isomer in the solutions, only the signals of the *trans-oxo-O* isomer may be observed in the NMR spectra. On the other hand, because the *trans-oxo-N* isomer has a lower solubility than the *trans-oxo-O* isomer, only the *trans-oxo-N* isomer may be obtained by crystallization from acetonitrile.[17]

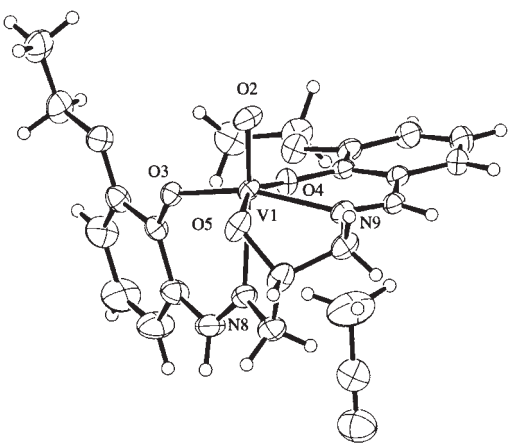

Fig. 2. ORTEP drawing of $[V^{V}O(L)]\cdot CH_3CN$ with 30% probability ellipsoids. Selected bond lengths (Å) and angles (°): V1–O2 1.599(2), V1–O3 1.877(1), V1–O4 1.890(1), V1–O5 1.863(2), V1–N8 2.241(2), V1–N9 2.110(2), O2–V1–N8 169.29(8).

Fig. 3. Two isomers of $[V^{V}O(L)]$.

Electrochemistry. Cyclic voltammograms of $[V^{V}O(L)]$ and $[V^{IV}O(HL)]$ are shown in Fig. 4. The voltammograms of $[V^{V}O(L)]$ in CH_2Cl_2, in CH_3CN, and in DMSO show a quasi-reversible V(V)/V(IV) redox couple with $E_{1/2} = -0.74$, -0.79, and -0.88 V, respectively (Fig. 4(a)). On the other hand, voltammograms of $[V^{IV}O(HL)]$ show a complicated redox process. The voltammogram in CH_2Cl_2 shows two irreversible oxidation waves at $+0.23$ and $+0.33$ V with a scan rate of 100 mV/s (Fig. 4(b)). The voltammogram in CH_3CN shows a redox couple with $E_{1/2} = +0.20$ V, and an irreversible oxidation wave at $+0.08$ V (Fig. 4(c)). The voltammogram in DMSO shows a quasi-reversible redox couple with $E_{1/2} = -0.05$ V (Fig. 4(d)). The voltammogram of $[V^{IV}O(HL)]$ in CH_2Cl_2 with a rapid scan (10 V/s) shows a redox couple with $E_{1/2} = +0.29$ V (Fig. 4(e)). There are two striking features in the voltammograms of $[V^{V}O(L)]$ and $[V^{IV}O(HL)]$. One is a large potential difference (ca. 1 V) between the V(V)/V(IV) redox couples of $[V^{V}O(L)]$ and $[V^{IV}O(HL)]$. The large potential difference may be explained by a different coordination environment around the vanadium atom. The ligand L in $[V^{V}O(L)]$ coordinates to the vanadium atom with the two imine

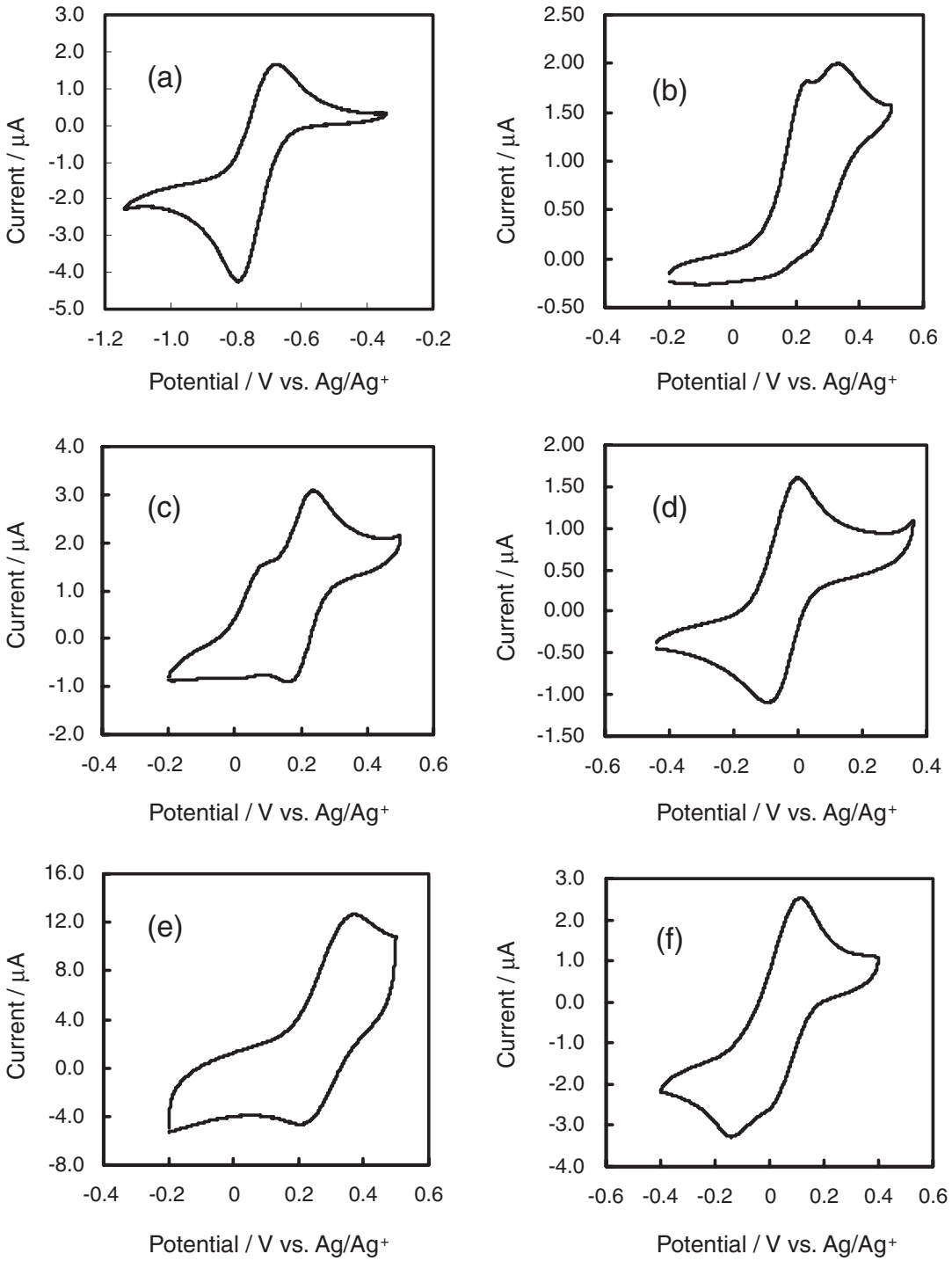

Fig. 4. Cyclic voltammograms of (a) $[V^{V}O(L)]$ in CH_2Cl_2 with a scan rate of 100 mV/s, (b) $[V^{IV}O(HL)]$ in CH_2Cl_2 with a scan rate of 100 mV/s, (c) $[V^{IV}O(HL)]$ in CH_3CN with a scan rate of 100 mV/s, (d) $[V^{IV}O(HL)]$ in DMSO with a scan rate of 100 mV/s, (e) $[V^{IV}O(HL)]$ in CH_2Cl_2 with a scan rate of 10 V/s, (f) $[V^{V}O(L)]$ with an equimolar amount of CF_3COOH in CH_3CN with a scan rate of 100 mV/s.

nitrogen, two phenolate oxygen, and alcoholate oxygen atoms. On the other hand, the ligand HL in $[V^{IV}O(HL)]$ coordinates to the vanadium atom with the two imine nitrogen and two phenolate oxygen atoms. The different coordination environment should effect the electronic conditions of the vanadium complexes. A voltammogram of $[V^{V}O(L)]$ with an equimolar amount of CF_3COOH in CH_3CN shows a V(V)/V(IV) couple around 0 V (Fig. 4(f)). The addition of acid to an CH_3CN solution of $[V^{V}O(L)]$ could cause protonation of the alcoholate group to yield the $[V^{V}O(HL)]^{+}$ species, which show a large positive shift of the redox potential. The other feature is a clear solvent dependence in the voltammograms of $[V^{IV}O(HL)]$. Although a quasi-reversible redox couple is observed in the voltammogram in DMSO, two irreversible oxidation waves are

observed in the voltammogram in CH_2Cl_2 with a scan rate of 100 mV/s. The absence of reduction waves in the voltammogram in CH_2Cl_2 indicates the presence of a chemical reaction following the oxidation process (EC reaction). The appearance of a redox couple by a rapid scan in the voltammogram in CH_2Cl_2 (Fig. 4(e)) inform restraint of the chemical reaction and the disappearance of one of the oxidation waves with a slow electron-transfer rate. These data indicate the presence of two different vanadium centers in a CH_2Cl_2 solution of $[V^{IV}O(HL)]$. In other words, $[V^{IV}O(HL)]$ may form dimeric species in CH_2Cl_2. In a strongly Lewis basic solution, such as DMSO, polymeric oxovanadium(IV) complexes with a tetradentate Schiff base ligand, like $[V^{IV}O(salpn)]$, are known to form a monomeric structure with weak coordination of a solvent molecule trans to the oxo atom.[10,18] $[V^{IV}O(HL)]$ will also form a monomeric structure in DMSO. However, in a weakly Lewis basic solvent, such as CH_2Cl_2, solvent molecules hardly coordinate to the vanadium atom, and the alcohol group of $[V^{IV}O(HL)]$ is supposed to coordinate to the vanadium atom of the adjacent molecule to form dimeric species.

To investigate the redox process of polymeric oxovanadium complexes, cyclic voltammetric measurements for $[V^{IV}O(3EtOsalpn)]$ {$H_2$3EtOsalpn: *N*,*N*′-bis(3-ethoxysalicylidene)-1,3-propanediamine} were carried out. $[V^{IV}O(3EtOsalpn)]$ has a similar structure to $[V^{IV}O(HL)]$, except for the alcohol group. $[V^{IV}O(3EtOsalpn)]$ also has a polymeric structure in the solid state (ν(V=O): 857 cm^{-1}),[10] and the complex is soluble in CH_2Cl_2 and in DMSO.[11] Cyclic voltammograms of $[V^{IV}O(3EtOsalpn)]$ are shown in Fig. 5. The voltammogram in CH_2Cl_2 shows a two-step redox reaction with the oxidation peaks at +0.32 and +0.49 V and the reduction peaks at +0.21 and +0.39 V (Figs. 5(a) and (b)). On the other hand, the voltammogram in DMSO shows a reversible V(V)/V(IV) redox couple with $E_{1/2} = -0.01$ V (Fig. 5(c)). The voltammogram in CH_2Cl_2 with a rapid scan (1 V/s and 10 V/s) shows a similar wave form to that with a scan rate of 100 mV/s, except for a broadening of the peaks.[19] There is a concentration dependence in the voltammograms in CH_2Cl_2. The voltammogram of the 2 mM complex shows two-step redox waves more clearly than that of the 1 mM complex (Figs. 5(a) and (b)). Thus, the redox process of $[V^{IV}O(3EtOsalpn)]$ in CH_2Cl_2 is different from that of $[V^{IV}O(HL)]$ in CH_2Cl_2. In DMSO, $[V^{IV}O(3EtOsalpn)]$ is also supposed to form a monomeric structure with weak coordination of a DMSO molecule. On the other hand, in CH_2Cl_2, the oxo atom of $[V^{IV}O(3EtOsalpn)]$ is supposed to coordinate to the vanadium atom of the adjacent molecule to form oligomers (···V=O···V=O···). The two-step redox process may have originated from an internuclear interaction between the vanadium centers in the oligomers.

The electronic spectra of the oxidized product of $[V^{IV}O(HL)]$, obtained by controlled potential oxidation at +0.5 V in CH_3CN, are shown in Fig. 6. Before the oxidation, the color of an CH_3CN solution of $[V^{IV}O(HL)]$ is brown, and the spectrum does not show any strong absorption bands in the range between 500 and 700 nm at a concentration of 0.5 mM (Fig. 6(a)). With progress of the oxidation reaction, the color of the solution turned dark blue, and a new band at 515 nm appeared (Fig. 6(b)). By standing the solution for 1 h following the oxidation reaction, the band peak at 515 nm shifted to

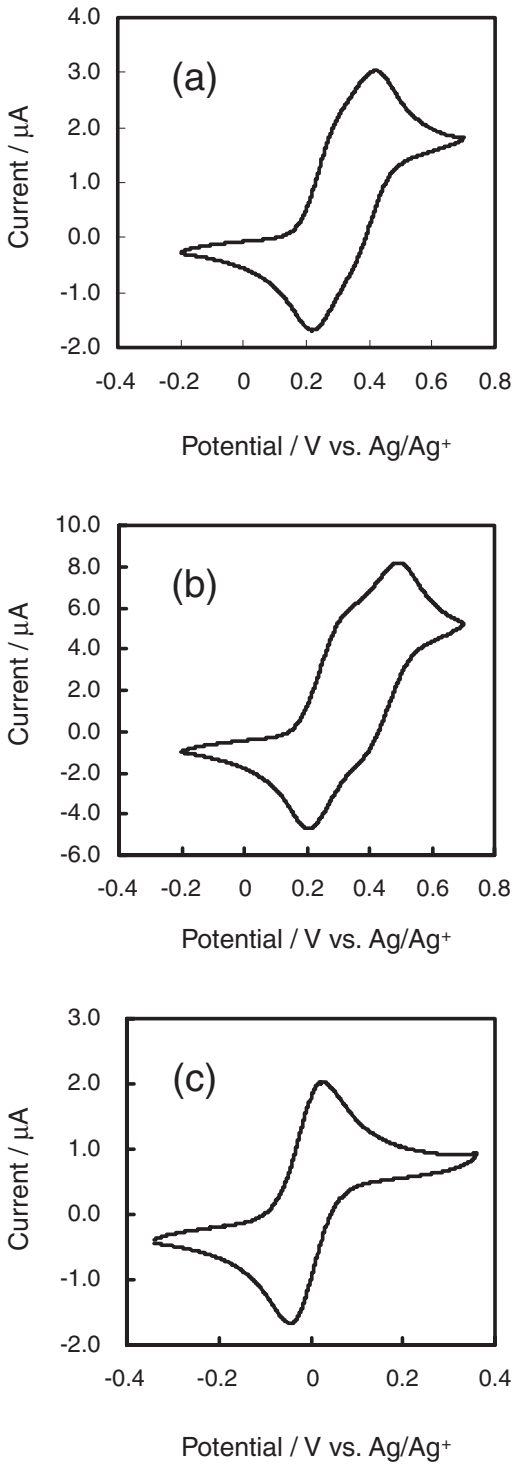

Fig. 5. Cyclic voltammograms of $[V^{IV}O(3EtOsalpn)]$ with a scan rate of 100 mV/s: (a) in CH_2Cl_2 with 1 mM complex, (b) in CH_2Cl_2 with 2 mM complex, (c) in DMSO with 1 mM complex.

534 nm (Fig. 6(c)). The band peak at 534 nm is almost coincident with that of $[V^{V}O(L)]$ in CH_3CN (535 nm). These results indicate the presence of a slow chemical reaction following the electrolytic oxidation reaction. The slow chemical reaction may include deprotonation of the alcohol group of $[V^{V}O(HL)]^+$ and coordination of the alcoholate group to the

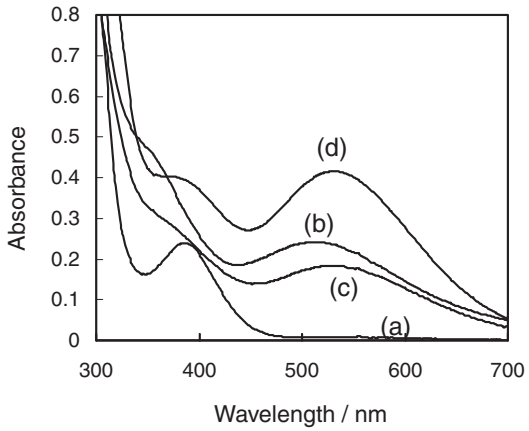

Fig. 6. Electronic spectra of the oxidized product of $[V^{IV}O(HL)]$, obtained by controlled potential oxidation at +0.5 V vs Ag/Ag^+ in CH_3CN: (a) before the oxidation reaction (0.5 mM complex), (b) just after the oxidation reaction, (c) after 1 h following the oxidation reaction, (d) spectrum of $[V^{V}O(L)]$ (1 mM complex).

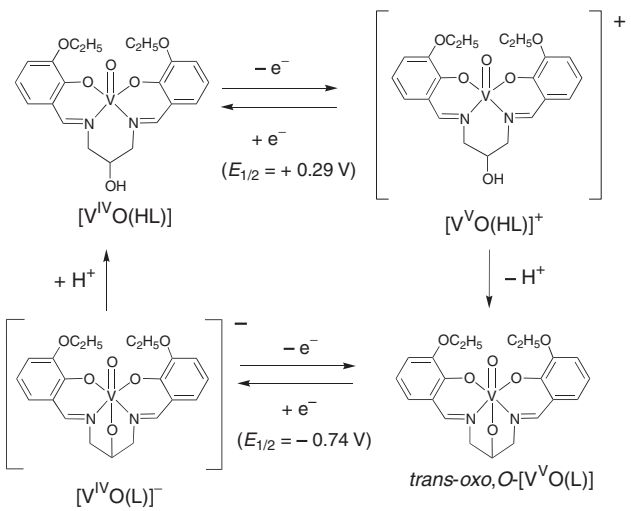

Fig. 7. Proposed mechanism for the redox reactions of $[V^{IV}O(HL)]$ and $[V^{V}O(L)]$.

vanadium atom (Fig. 7).

In the present study, new oxovanadium(IV) and (V) complexes with a pentadentate Schiff base ligand, $[V^{IV}O(HL)]$ and $[V^{V}O(L)]$ were prepared, and their structures and electrochemical properties were investigated. The proposed mechanism for the redox reactions of the complexes are summarized in Fig. 7.

Experimental

Preparation of the Ligand. The ligand H_3L was prepared by the reaction of 2-hydroxy-1,3-propanediamine with 2 equiv amounts of 3-ethoxy-2-hydroxybenzaldehyde in ethanol. The reaction mixture was evaporated to dryness to yield a yellow oily product. The oily product was poured into water, and the mixture was stirred for 1 d. The resulting yellow powder was collected by filtration and used for further reactions without purification. ^{13}C NMR ($CDCl_3$) δ 167.3, 152.8, 147.8, 123.4, 118.5, 117.8, 115.8 (Ar and N=CH–C), 70.2 (–OCH(CH_2–)$_2$), 64.5 (O–CH_2–C), 62.2 (N–CH_2–C), 14.9(CH_3).

$[V^{IV}O(HL)]\cdot H_2O$. $[V^{IV}O(acac)_2]$ (1.33 g, 5 mmol) and the ligand H_3L (1.93 g, 5 mmol) were added to 100 cm^3 of CH_3CN under an argon atmosphere. The reaction mixture was stirred at 30 °C for 1 h to yield a brown precipitate. The brown product was collected by filtration, and washed with acetonitrile. Yield: 1.83 g (78%). Found: C, 53.94; H, 5.62; N, 5.86%. Calcd for $C_{21}H_{26}N_2O_7V_1$: C, 53.74; H, 5.58; N, 5.97%.

$[V^{V}O(L)]\cdot CH_3CN$. $[V^{IV}O(acac)_2]$ (1.33 g, 5 mmol) and the ligand H_3L (1.93 g, 5 mmol) were added to 200 cm^3 of dry CH_3CN in air. At first, a brown powder was precipitated from the reaction mixture. However, the precipitation was gradually dissolved in CH_3CN, and the color of the solution turned dark blue upon stirring for 3 h at 60 °C. After filtration, the reaction mixture was left for one day. Dark-blue crystals of $[V^{V}O(L)]\cdot CH_3CN$ were collected by filtration, and washed with a small amount of CH_3CN. Yield: 1.47 g (60%). Found: C, 56.06; H, 5.49; N, 8.21%. Calcd for $C_{23}H_{26}N_3O_6V_1$: C, 56.22; H, 5.33; N, 8.55%. Prismatic single crystals were used for X-ray crystal structure analysis.

Crystal Structure Determination of $[V^{V}O(L)]\cdot CH_3CN$. Crystal data of $[V^{V}O(L)]\cdot CH_3CN$: $V_1O_6N_3C_{23}H_{26}$, $M = 491.42$, crystal size: $0.68 \times 0.40 \times 0.20$ mm, monoclinic, space group $P2_1/a$ (No. 14), $a = 21.788(4)$, $b = 10.996(3)$, $c = 10.078$ Å, $\beta = 102.92(1)^\circ$, $V = 2353.3(8)$ Å^3, $Z = 4$, μ(Mo Kα) = 0.464 mm^{-1}, 6253 reflections measured, 5414 independent reflections. The intensity data were collected at 298 K on a Rigaku AFC-7R diffractometer with graphite-monochromatized Mo Kα radiation ($\lambda = 0.71073$ Å) up to $2\theta = 55^\circ$ by ω scans. Three standard reflections were measured at every 150 reflections. Absorption corrections were made by the Ψ scans method.[20] The structures were solved by direct methods on a Silicon Graphics O^2 workstation with the program system TEXSAN,[21] and refined with SHELXL-97.[22] Non-hydrogen atoms were treated anisotropically, and hydrogen atoms attached to the carbon atoms were introduced at ideal positions. The refinement was based on F^2 with $R_w = [\Sigma w(F_o^2 - F_c^2)^2/\Sigma w(F_o^2)^2]^{1/2}$, $w^{-1} = \sigma^2(F_o^2) + (0.0490P)^2 + 0.9117P$, where $P = (F_o^2 + 2F_c^2)/3$ against all of the 5414 reflections. The R_w value was 0.108. The R value $(\Sigma|F_o^2 - F_c^2|/(\Sigma F_o^2)$ was 0.038 for the 3966 reflections with $I > 2\sigma(I)$. Crystallographic data have been deposited at the CCDC, 12 Union Road, Cambridge CB2 1EZ, UK and copies can be obtained on request, free of charge, by quoting the publication citation and the deposition numbers CCDC 244791 and 244792.

Electrochemical Measurements. Cyclic voltammetric measurements were carried out using a ALS 600 electrochemical analyzer at 25 °C (1 mM complex, 0.1 M $N(C_4H_9)_4BF_4$). A platinum electrode, an Ag/Ag^+ electrode (Ag/0.01 M $AgNO_3$), and a platinum wire were employed as the working, reference, and auxiliary electrodes, respectively. As an external standard, the redox potential of the Fc^+/Fc (Fc: ferrocene) couple in CH_3CN was observed at +0.043 V vs Ag/Ag^+ under these conditions. The controlled potential oxidation of $[V^{IV}O(HL)]$ with a Pt mesh electrode was carried out at +0.5 V vs Ag/Ag^+ in CH_3CN under a nitrogen atmosphere (0.5 mM complex, 0.1 M $N(C_4H_9)_4BF_4$). The progress of the oxidation reaction was monitored with the current values.

Other Measurements. The IR spectra were recorded on a JASCO FT/IR-230 spectrophotometer. The ^1H and ^{13}C NMR spectra were recorded on JEOL JNM-GX400 and BRUKER AVANCE 400 spectrometers with a TMS reference.

The present work was supported in part by Grant-in-Aid for Scientific Research No. 15550055 from the Ministry of Education, Culture, Sports, Science and Technology.

References

1 A. Pasini and M. Gullotti, *J. Coord. Chem.*, **3**, 319 (1974).

2 M. Mathew, A. J. Carty, and G. J. Palenik, *J. Am. Chem. Soc.*, **92**, 3197 (1970).

3 L. Banci, A. Bencini, A. Dei, and D. Gatteschi, *Inorg. Chim. Acta*, **84**, L11 (1984).

4 J. A. Bonadies, W. M. Butler, V. L. Pecoraro, and C. J. Carrano, *Inorg. Chem.*, **26**, 1218 (1987).

5 M. Tsuchimoto and S. Ohba, *Acta Crystallogr., Sect. C*, **55**, IUC9900008 (1999).

6 M. Tsuchimoto, E. Yasuda, and S. Ohba, *Chem. Lett.*, **2000**, 562.

7 E. Tsuchida, K. Yamamoto, K. Oyaizu, N. Iwasaki, and F. C. Anson, *Inorg. Chem.*, **33**, 1056 (1994).

8 K. Nakajima, K. Kojima, M. Kojima, and J. Fujita, *Bull. Chem. Soc. Jpn.*, **63**, 2620 (1990).

9 M. Tsuchimoto, G. Hoshina, R. Uemura, K. Nakajima, M. Kojima, and S. Ohba, *Bull. Chem. Soc. Jpn.*, **73**, 2317 (2000).

10 M. Tsuchimoto, R. Kasahara, K. Nakajima, M. Kojima, and S. Ohba, *Polyhedron*, **18**, 3035 (1999).

11 Most of polymeric oxovanadium(IV) complexes with a tetradentate Schiff base ligand are scarcely soluble in organic solvents except for DMSO and DMF. For the polymeric oxovanadium(IV) complexes, cyclic voltammograms only in DMSO have been reported.

12 K. Yamamoto, K. Oyaizu, and E. Tsuchida, *J. Am. Chem. Soc.*, **118**, 12665 (1996).

13 D. L. Hugh, U. Kleinkes, G. J. Leigh, M. Maiwald, J. R. Sanders, and C. Sudbrake, *J. Chem. Soc., Dalton Trans.*, **1994**, 2457.

14 K. Oyaizu, K. Yamamoto, K. Yoneda, and E. Tsuchida, *Inorg. Chem.*, **35**, 6634 (1996).

15 E. Tsuchida and K. Oyaizu, *Coord. Chem. Rev.*, **237**, 213 (2003).

16 ^{1}H and ^{13}C NMR spectra of $[V^{V}O(L)]$ in CD_2Cl_2 are deposited as Document No. 04055 at the Office of the Editor of Bull. Chem. Soc. Jpn. The ^{13}C NMR spectrum of $[V^{V}O(L)]$ shows several very small unidentified signals besides the signals of the complex. These unidentified signals are assigned to the signals of the decomposed products formed during the overnight measurement.

17 Reaction of the ligand H_3L with $[V^{IV}O(acac)_2]$ in dry CH_3OH in air yielded needle crystals of $[V^{V}O(L)]$, which had no solvent of crystallization. Yield: 44%. Found: C, 55.79; H, 5.09; N, 6.29%. Calcd for $C_{21}H_{23}N_2O_6V_1$: C, 56.01; H, 5.15; N, 6.22%. Crystal data of $[V^{V}O(L)]$: $V_1O_6N_2C_{21}H_{23}$, $M = 450.36$, crystal size: $0.68 \times 0.20 \times 0.09$ mm, orthorhombic, space group *Pbca* (No. 61), $a = 20.007(9)$, $b = 18.470(7)$, $c = 11.483(4)$ Å, $V = 4243(3)$ Å^3, $Z = 8$, $\mu(\mathrm{Mo\,K}\alpha) = 0.507$ mm^{-1}, 5760 reflections measured, 4869 independent reflections. $R = 0.046$ against the 2814 reflections with $I > 2\sigma(I)$, $R_w = 0.142$ against all the 4869 reflections. The structure of the complex in the crystals of $[V^{V}O(L)]$ is almost identical with that in the crystals of $[V^{V}O(L)]\cdot CH_3CN$.

18 C. A. Root, J. D. Hoeschele, C. R. Cornman, J. W. Kampf, and V. L. Pecoraro, *Inorg. Chem.*, **32**, 3855 (1993).

19 Cyclic voltammograms of $[V^{IV}O(3EtOsalpn)]$ in CH_2Cl_2 with a scan rate of 1 V/s and 10 V/s (1 mM complex) are deposited as Document No. 04055 at the Office of the Editor of Bull. Chem. Soc. Jpn.

20 A. C. T. North, D. C. Phillips, and F. S. Mathews, *Acta Crystallogr.*, **A24**, 351 (1968).

21 "TEXSAN, Version 1.11, Single crystal structure analysis software," MSC, 9009 New Trial Drive, The Woodlands, TX 77381, U.S.A., Rigaku, 3-9-12 Akishima, Tokyo 196-8666, Japan.

22 G. M. Sheldrick, "SHELXL97: Program for the Refinement of Crystal Structures," University of Göttingen, Germany (1997).